  Bull. Chem. Soc. Jpn., 56, 1598—1606 (1983) [Vol. 56, No. 6

Association of Chlorophyll with Amides on Plasticized Polyethylene Particles. II. The Isomeric *N*-Pyridylmyristamides

Yoshihumi Kusumoto,*,† Gilbert R. Seely, and Velu Senthilathipan
Charles F. Kettering Research Laboratory, Yellow Springs, Ohio 45387 U.S.A.
(Received October 12, 1982)

When chlorophyll, together with certain other amphiphilic substances, is adsorbed to particles of polyethylene plasticized by incorporation of tetradecane, it is maintained in monomeric or oligomeric forms with characteristic absorption and fluorescence spectra. The present work describes the properties of chlorophyll a on such particles in the presence of the three isomeric *N*-pyridylmyristamides, and of the similarly shaped but not basic compound myristanilide, in an effort to ascertain the structural factors governing associations of these species. Absorption and fluorescence spectra at room temperature are resolved into minimal sets of Gaussian components, and relations between the component sets are proposed. The positions of the component bands and their relative abundance are characteristic of the amide used. The 3- and 4-pyridyl isomers bind more strongly to chlorophyll, probably by ligation of the pyridine nitrogen to Mg of the pigment. The 2-pyridyl isomer and myristanilide bind more weakly, probably through the amide carbonyl group. The association of chlorophyll into species with characteristic absorption and fluorescence bands is promoted more strongly by the 3- and 4-isomers than by the 2-isomer and myristanilide, and probably involves hydrogen bonding to chlorophyll carbonyl groups. A possible manner of association of chlorophyll in the presence of *N,N*-dimethylmyristamide is also presented. By way of comparison, chlorophyll adsorbed with *N*-dodecylpyridinium bromide, which lacks a nucleophilic function, is mainly in the microcrystalline hydrate form absorbing near 740 nm.

Preliminary accounts of this subject have reported the association of chlorophyll a with a number of amphiphilic amides when both are adsorbed to polyethylene particles swollen by absorption of a hydrocarbon diluent such as undecane.[1] The previous paper in this series (I) presented in some detail the evidence for interaction of chlorophyll with *N,N*-dimethylmyristamide (DMMA) adsorbed to swollen polyethylene.[2a] In the presence of sufficient DMMA, chlorophyll is maintained in monomeric and associated species with characteristic absorption and fluorescence spectral bands. The associated as well as the monomeric species were apparently capable of strong fluorescence even at chlorophyll densities corresponding to monolayer coverage, and photochemical activity was demonstrated.

We have also examined the interaction of chlorophyll with the closely related amphiphile *N*-methylmyristamide, and found quite different sorts of chlorophyll association.[2b] In this paper we report the association of chlorophyll with certain other *N*-monosubstituted amphiphilic amides, specifically the three isomeric *N*-pyridylmyristamides (NPMA's). These substances were chosen principally for two reasons. First, since the pyridine nitrogen function, like the amide carbonyl, is known to bind to the Mg of chlorophyll, we might find evidence for association of chlorophyll through either or both functions, depending on the isomer. Second, the pyridine chromophore provides a convenient means of accurately estimating the amphiphile concentration in the particle preparations, which is lacking for entirely aliphatic amides. We further include for comparison preparations with myristanilide (MAn), which resembles the NPMA's in shape but lacks pyridine nitrogen, and with *N*-dodecylpyridinium bromide (DPB), a surfactant made from pyridine which has no Lewis base function capable of binding to chlorophyll.

† Present address: Chemical Institute, College of Liberal Arts, Kagoshima University, Korimoto, Kagoshima 890.

Experimental

Materials. The isomeric *N*-pyridylmyristamides were prepared by reaction of the corresponding aminopyridines with myristoyl chloride in acetone or *N,N*-dimethylformamide, similarly to the procedure of Deady and Stillman,[3] and were purified by reprecipitation from methanol–aqueous ammonia. Myristanilide was prepared by reaction of myristoyl chloride with aniline in toluene containing triethylamine, and recrystallized finally from ethanol. *N*-Dodecylpyridinium bromide was prepared by refluxing pyridine with 1-bromododecane in toluene.

N-*(2-Pyridyl)myristamide*: IR (KBr): 3355 (N–H), 1698 (amide I), 1538 (amide II), 1590, 1447, and 778 cm^{-1} (pyridyl). UV_{max} (1-propanol): 276 (ε, 5670) and 236 nm (10360). Found: C, 74.70; H, 10.93; N, 8.84%. Calcd for $C_{19}H_{32}N_2O$: C, 74.95; H, 10.59; N, 9.20%.

N-*(3-Pyridyl)myristamide*: Mp 80.5—82 °C. IR (KBr): 3331, 1676, 1543, 1597, 1423, 802, and 707 cm^{-1}. UV_{max} (1-propanol): 279 (4400) and 241 nm (16450). Found: C, 75.48; H, 11.40; N, 9.07%.

N-*(4-Pyridyl)myristamide*: Mp 75—77 °C. IR (KBr): 3428, 1686, 1534, 1615, 1427, and 834 cm^{-1}. UV_{max} (1-propanol): 246.5 nm (17790). Found: C, 73.28; H, 10.79; N, 8.62%.

Myristanilide: Mp 84.5—85 °C. IR: 3312, 1670, 1549 (amide), and 1612, 1454, 759, 696 (phenyl). UV_{max} (1-propanol): 243 nm (16310).

N-*Dodecylpyridinium Bromide*: IR: 1650, 1497, 782, and 691 cm^{-1} (pyridinium). UV_{max}: 260 nm (4660).

Methods. The polyethylene particles swollen with tetradecane were prepared as described.[2] Tetradecane was used as diluent instead of undecane, as in (I), primarily because of its lower solubility in aqueous methanol. The swollen particles contained about 75% tetradecane. The adsorption of chlorophyll and amide from aqueous methanol was performed as described in (I), but because of their low solubility in 60% methanol, the amides were present only in the initial 90% methanol solution, along with chlorophyll. Chlorophyll and amphiphile contents of the recovered particles were estimated spectrophotometrically on a 1-propanol extract of a sample of particles. The uptake of amide by the particles is linear

with concentration at low values thereof, and their concentrations on the particles, $[NPMA]_p$, are related to their concentrations in 75% methanol solution ([NPMA]) by Eqs. 1—4.

$$[4\text{-NPMA}]_p/\mu\text{mol g}^{-1} = 0.84([4\text{-NPMA}]/\text{mM}),^{\dagger\dagger} \quad (1)$$

$$[3\text{-NPMA}]_p = 0.93[3\text{-NPMA}], \quad (2)$$

$$[2\text{-NPMA}]_p = 11.9[2\text{-NPMA}], \quad (3)$$

$$[\text{MAn}]_p = 48[\text{MAn}]. \quad (4)$$

Above 2.5 mM [3-NPMA] and about 1.5 mM [2-NPMA] or [MAn], the amount of amide bound to the particles exceeded that predicted by the equations, because of precipitation out of 75% methanol or multilayer adsorption. The proportionality constants suggest that 3-NPMA and 4-NPMA are adsorbed only to the particle surface, while MAn and 2-NPMA are dissolved in the particles to some extent. The solubility of 2-NPMA is perhaps owing to the formation of a cylic dimer, like that of 2-aminopyridine in CCl_4 solution.[4]

Absorption Spectroscopy. Absorption spectra were recorded on a Perkin-Elmer Hitachi 557 spectrophotometer, of mixtures not exceeding 2% (wt) of green particles with a densely scattering white paste. At these concentrations, the absorbance is proportional to the relative absorptivity, and the expected optical path enhancement by multiple scattering is observed.[5]

The pastes usually consist of three components: (1) a fluid, normally a non-solvent for chlorophyll such as water or glycerol; (2) a thickener, often a polysaccharide, to keep the particles in suspension; (3) an inert scattering material such as cellulose (Sigmacell, 20 μm particles). Two pastes that have proved useful in absorption spectroscopy are water (43.3%), Ficoll 400 (Pharmacia) (28.9%), cellulose (27.8%), and water (25.8%), sucrose (51.7%), cellulose (22.5%). For fluorescence spectroscopy a paste (CGW) of Carbowax PEG-1000 : glycerol : water (10 : 11 : 1 in wt/v/v) was used, so that the sample could be cooled to 77 K. A paste (OCC) which extracts chlorophyll from the particles was compounded out of 1-octanol (42.4%), Carbowax PEG 1500 (18.3%) and cellulose (39.3%). For recording spectra, the pastes were spread in an even layer 0.10 cm deep in a demountable silica cell. Second derivative absorption spectra were also recorded.

Fluorescence Spectroscopy. Most fluorescence spectra discussed here were recorded from the front surface of a thin layer of particles mixed with CGW paste, first at room temperature then after quickly cooling with liquid nitrogen.

Exciting light was provided by a Sylvania 250-W Q/CL/DC tungsten-halogen lamp and dispersed by a Beckman DU monochromator. It was focused on the sample surface at an angle of about 15° to the normal. The fluorescence was dispersed by a Spex 0.5 m Czerny-Turner monochromator, with 64×64 mm grating, 1200 grooves/mm, blazed for 750nm, and turned by a Minidrive stepping motor. The rated dispersion was 1.6 nm/mm, and it was usually operated with 1 mm slits.

The fluorescence was detected with a Hamamatsu R666 GaAs photomultiplier at 1000 V; the signal was amplified by a Keithley 610 B Electrometer and recorded on a Kipp and Zonen BD 12 Intergrating Recorder. The apparatus was calibrated for variation of sensitivity with wavelength by means of a tungsten lamp operated at different color temperatures.

Analysis of Spectra. Absorption spectra, and fluorescence spectra corrected for variation of sensitivity with wavelength, were resolved into Gaussian component bands with the aid of an IBM 5100 portable computer. Two programs were used. For absorption spectra, where the band positions (λ) are close together and there was little direct evidence for the value of the component bandwidths (B) at half peak height, all trial bandwidths were assumed to have the same value. This program found the trial band heights and the value of B which simultaneously fitted the spectrum at the N band positions, and minimized the sum of deviations at $N+1$ other points on the spectrum. The calculated spectrum was compared with the observed at about 30 points spaced 2 nm apart, and trial band positions were adjusted to remove any systematic deviations. If no further adjustment could return a satisfactory fit, one more band was added and the process was repeated.

For all fluorescence spectra and some absorption spectra the assumption of identical B was plainly invalid. The program in these cases assumed trial values of λ and B for each band, and calculated band heights to match the observed spectrum at the N band positions. Band positions and widths were varied individually, and bands added if necessary, until acceptable fit was obtained to the observed spectrum.

So far as possible, only bands identified as peaks or shoulders in the absorbance or fluorescence spectrum, or as troughs or shoulders in the second derivative spectrum, were included as trial bands in the analysis. A minimal number of other components were introduced only when resolution based on identified bands was unsatisfactory. Furthermore, the bandwidth of components located at $\lambda<720$ nm was not allowed to exceed 24 nm, approximately the maximum value observed under any circumstances for monomeric chlorophyll.[6]

An inherent limit to the precision of spectral reconstruction is the non-Gaussian shape of the chlorophyll band itself. However, the absorption spectrum of chlorophyll in acetone could be fitted by one Gaussian ($\lambda=661.7$ nm, $B=20.6$ nm) within 1% of peak height from 652 to 680 nm, and within 2% to 710 nm. Similar precision was accepted as evidence of satisfactory fit for the particle sample spectra. As a further test of acceptability, a single set of bands (λ, B within ± 1 nm) should fit the spectra of all particles prepared with chlorophyll and a given surfactant. To a surprising extent these criteria have been met in the systems under discussion. In practice, the reconstructed spectrum proved sensitive to variations of $\pm(0.5—1)$nm in component band position and width, so that we have reasonable confidence in our representations.

Results

Chl in OCC. When green particles are mixed with this paste, chlorophyll is dissolved from them by the 1-octanol component. Absorption and fluorescence spectra (Fig. 1) are therefore of monomeric chlorophyll in a highly scattering solution and serve as a standard for comparison with chlorophyll adsorbed to particles in a highly scattering suspension. The absorption band can be represented well enough by one Gaussian component at 665.8 nm, with bandwidth $B=24$ nm. The fluorescence at room temperature is well represented by three components, at 680 nm ($B=23$ nm) 57.3%, 702 nm (20 nm) 9.0%, and 732 nm (40 nm) 33.8%, where the percentages represent the fraction of the integrated fluorescence intensity contributed by the component. The last two components are separated from the first by 450 and 1040 cm^{-1}, which perhaps correspond to pyrrole ring deformation and pulsation frequencies. At 77 K the same three components are present, with slightly altered contributions: 680(20)

†† 1 M=1 mol dm^{-3} and 1 mM=1×10^{-3} mol dm^{-3} in this paper.

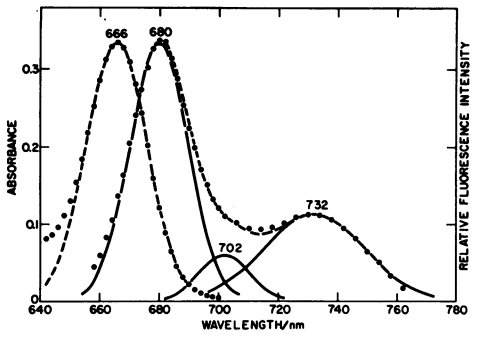

Fig. 1. Absorption and fluorescence spectra (the latter normalized at the 680-nm peak to match the absorption band) of chlorophyll-containing particles ($[Chl]_p$= 1.046 μmol g^{-1}) suspended in a paste of 1-octanol (42.4%), Carbowax 1500 (18.3%), and cellulose (39.3%) (OCC), in which chlorophyll is soluble. The particles were prepared with a concentration of 3-NPMA so low (0.625×10^{-3} M) that most of the chlorophyll was in the form of the microcrystalline hydrate absorbing around 740 nm (see Fig. 2). The disappearance of that band shows that the chlorophyll has dissolved in the OCC paste. For the absorption spectrum, 0.0109 g of green particles was blended with 0.721 g of OCC paste; for the fluorescence spectrum, 0.1235 g of particles with 0.300 g OCC paste. The red band of the absorption spectrum is represented adequately by one Gaussian component (dashed curve), the fluorescence spectrum by three. The fluorescence components are shown as solid traces, their sum as a dashed trace. Observed absorption and fluorescence intensities, the latter corrected for variation of instrumental sensitivity with wavelength, are plotted as open circles.

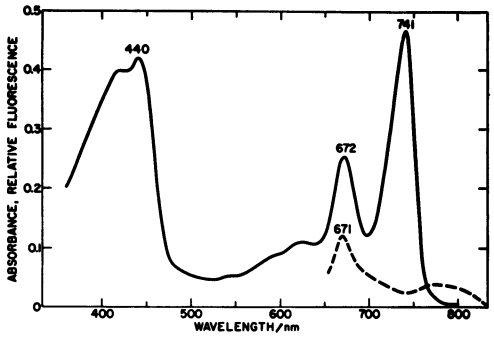

Fig. 2. Visible absorption and fluorescence spectra of particles containing chlorophyll (1.36 μmol g^{-1}) and DPB (2.66 μmol g^{-1}), the latter adsorbed from a 5 mM solution, initial concentration. For absorption spectral measurement, 0.0141 g of yellow-green particles was mixed with 0.578 g of a paste of Ficoll (39%), cellulose (Sigmacell, 15%), and water (46%). The paste scattering background has been subtracted. For fluorescence (dashed trace), 0.0585 g of particles was mixed with 0.255 g of the paste, and excited at 616 nm. There is indication of reabsorption by the strong 741 nm absorption band. The weak fluorescence was not corrected for variation of apparatus sensitivity to wavelength, because of uncertainty in the location of the baseline.

48.1%, 702(20) 9.4%, and 734(40) 42.6%.

Although there is little reason to doubt that chlorophyll is monomeric in this system, the Stokes shift (14 nm), and the 732 nm fluorescence vibronic component, are large in comparison with those of other spectra we have recorded, *i.e.*, chlorophyll in acetone, or in undecane solution with DMMA.[2] The absorption bandwidth (24 nm) is larger than twice the half-bandwidths in any of the solvents reported previously by Seely and Jensen.[6] The broadening and red-shifting are perhaps consequences of strong hydrogen-bonding between octanol and chlorophyll carbonyls in the ground and excited states.[7] The mirror-image relation between absorption and fluorescence bands is obvious, which incidentally demonstrates that reabsorption of fluorescence is not a domineering phenomenon in our systems.

N-*Dodecylpyridinium Bromide.* This surfactant is not basic and therefore does not bind to functional groups of chlorophyll. In sharp contrast to the foregoing spectra, the spectrum of chlorophyll (1.359 μmol g^{-1}) with DPB (2.66 μmol g^{-1}, from 5 mM DPB in solution initially) in Fig. 2 show mainly the microcrystalline hydrate form of the pigment (741 nm). The same form appears when chlorophyll is adsorbed to the particles in the absence of an amphiphile[2] and in many other systems where water is present.[8] The fluorescence is weak; the most prominent band in its spectrum (671 nm) probably corresponds to a small amount of monomeric chlorophyll absorbing around 662 nm. No attempt was made to resolve these spectra into components.

The presence of DPB does not prevent chlorophyll from associating with 3-NPMA on the same particle. Particles prepared with [DPB] and [3-NPMA], both 10 mM initially, and having the composition $[Chl]_p$= 1.212, $[DPB]_p$=1.55, and $[3\text{-NPMA}]_p$=5.32 μmol g^{-1}, had the same absorption and fluorescence spectra as chlorophyll in the presence of 3-NPMA alone (see below).

N-*(2-Pyridyl)myristamide.* As increasing amounts of an amphiphile such as 2-NPMA are present in solution to be adsorbed along with chlorophyll, the amount of chlorophyll in the 741 nm hydrated form decreases, and the amount in forms absorbing at shorter wavelengths increases. At sufficiently high amphiphile concentration, the 741 nm form of chlorophyll disappears altogether from the green particles. In Figs. 3—5, spectra of adsorbed chlorophyll with the three isomeric NPMA's are compared at $[Chl]_p$ around 1 μmol g^{-1}, and at a high enough NPMA concentration to eliminate the 741 nm species. In the absorption spectra, only the longest-wave, "red" band is shown and analysed; the remainder of the visible spectrum superficially resembles that of normal monomeric chlorophyll in a non-hydroxylic solvent. Differences seen at other chlorophyll and NPMA concentrations will be noted. Second derivative spectra generally show a sharper and more complex band system throughout the visible than is seen in the spectrum of chlorophyll in acetone, for example.

Spectra with 2-NPMA appear the easiest to interpret. At high amphiphile concentration the red absorption

band is resolved into two components, both relatively broad (Fig. 3a). The major one (666 nm) falls in the wavelength range expected for a monomeric chlorophyll species, but the minor one (684 nm) must represent some associated species, probably dimeric in chlorophyll. The fluorescence spectrum (Fig. 3b) is resolved into five components. Comparison with Fig. 1 suggests that the 693 nm component represents fluorescence from the 684 nm species in the absorption spectrum; the 1132 cm^{-1} interval between the 693 and 752 nm components, and their relative strength, suggest that the 752 nm component is a vibrational satellite of the other. Apart from these two bands, the fluorescence spectrum resembles that of monomeric chlorophyll in Fig. 1 (with a $\approx$6 nm blue shift), but the 726.5 nm component is distinctly stronger in the 2-NPMA spectrum.

At lower chlorophyll concentration ($[Chl]_p$=0.23 μmol g^{-1}), the spectra were quite similar to the foregoing,

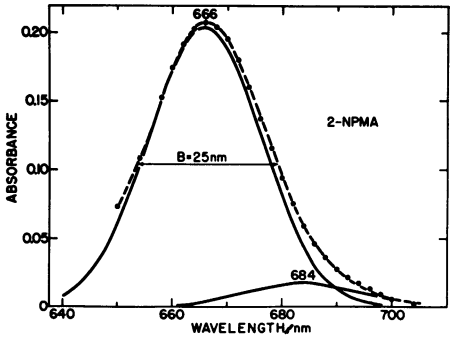

Fig. 3a. Absorption spectrum of particles containing chlorophyll (1.029 μmol g^{-1}) and 2-NPMA (68 μmol g^{-1}) in Ficoll–cellulose paste (0.0063 g green particles mixed with 0.603 g paste). The red band is most simply represented as the sum of two Gaussian components (solid traces), both 24 nm in bandwidth. Observed absorbances are plotted as open circles.

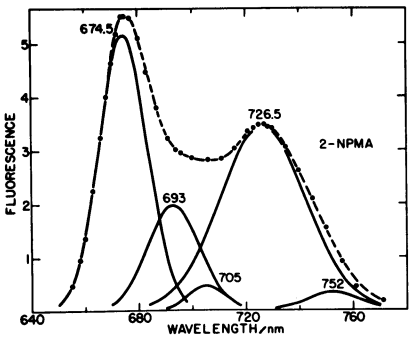

Fig. 3b. Fluorescence spectrum at room temperature of particles of Fig. 3a., 0.0794 g mixed with 0.191 g of CGW paste, under excitation at 600 nm. The spectrum is resolved into five components (solid traces): 674.5 nm (B=21 nm) 36.1%, 693(23) 15.2%, 705(16) 2.4%, 726.5(38) 43.7%, and 752(24) 2.5%. The sum of these is represented as a dashed trace, and observed fluorescence intensities are plotted as open circles. Compared to Fig. 1, there is more evidence of emission in longer-wavelength bands, indicating the presence of associated chlorophyll species.

but the monomer (674.5 nm) fluorescence component was greater (47.4%), and the 693 and 726 nm component contributions were smaller.

At 2-NPMA concentrations of 28 μmol g^{-1} or less, some of the chlorophyll remains in the 741 nm form. Now, a third component at 673.5 nm must be included to resolve the red band; *e.g.*, for $[Chl]_p$=1.10 and $[2\text{-NPMA}]_p$=28 μmol g^{-1}, the band was resolved into components at 666 nm (B=24 nm) 68.5%, 673.5(22) 29.2%, and 684(20) 2.3%. The fluorescence spectrum was not much different from that of Fig. 3b, and contained no component clearly corresponding to the 673.5 nm absorption component. This component may therefore represent the same species as the 672 nm band in Fig. 2. At 77 K the monomer fluorescence band at 674 nm was suppressed and replaced by a band in the 683—687 nm region. This band may reflect the 673.5 nm absorption component, or it may arise from a species formed on cooling the particles.

Myristanilide. This amphiphile resembles the NPMA's in shape but lacks the pyridine base function. Even more than 2-NPMA, it is soluble in the plasticized polyethylene particles and a fairly high concentration is needed to suppress the 741 nm chlorophyll species. Not many preparations have been examined with this amphiphile, but those that have show relatively simple absorption and fluorescence spectra, resembling those with 2-NPMA. The red absorption band of a preparation with $[Chl]_p$=0.974 and $[MAn]_p$=66.6 μmol g^{-1} in Ficoll–glycerol–cellulose paste is simple, but too broad (29 nm) to be represented by one Gaussian with $\leq$24 nm bandwidth. It was resolved satisfactorily into three components, at 658 nm (19.6%), 671 (64.7%), and 680.5 (15.7%), all with B=24 nm. However, the band is rather smooth and there are few clues to guide the selection of trial component wavelengths. The shape of the second derivative suggests that there may be four components in the red band region, and resolution into 655 nm (11.5%), 665 (34.8%), 674 (37.5%), and 682.5 (16.2%), all with B=20 nm, was also satisfactory. The fluorescence spectrum of the same preparation in CGW paste was resolved into four components, at 676 nm (B=24 nm) 52.1%, 697.5(20) 9.4%, 723.5(40) 33.3%, and 765(32) 5.2%. Except for the last component, the spectrum closely resembles that of monomeric chlorophyll in OCC, but displaced a few nm to the blue. At 77 K, the leading fluorescence band appears at 685 nm.

N-*(4-Pyridyl)myristamide.* The absorption spectrum resembles that with 2-NPMA but the red band, now at 668 nm, is broader. Two of three preparations showed a distinct shoulder in the second derivative spectrum around 684 nm, identifying a component there. The red band could not be resolved into two or even three bands of acceptable bandwidth as was done with the 2-NPMA preparations; a satisfactory resolution into four principal bands and a fifth, small band at 697.5 nm is presented in Fig. 4a. It was necessary to include a component (656 nm) at a shorter wavelength than the presumed monomer component band (666 nm), to represent the broadened short-wave side of the absorption band. The spectrum of a preparation with $[Chl]_p$=

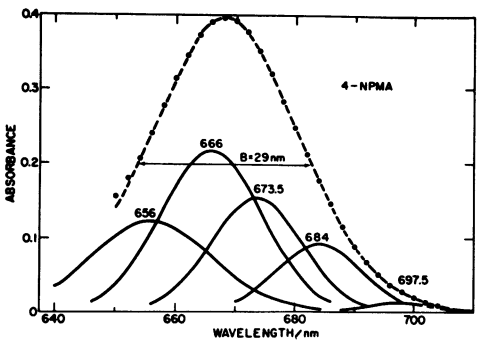

Fig. 4a. Absorption of particles containing chlorophyll (1.142 μmol g^{-1}) and 4-NPMA (4.18 μmol g^{-1}), 0.0082 g of green particles mixed with 0.608 g of Ficoll–cellulose paste. The broad red band is resolved into five components (solid traces): 656 nm (B=24 nm) 24.8%, 666(20) 37.0%, 673.5(18) 23.6%, 684(17) 13.2%, and 697.5(13) 1.4%. Their sum is shown as a dashed line, and observed absorbances are plotted as open circles.

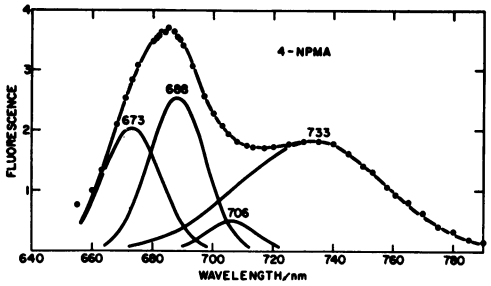

Fig. 4b. Fluorescence spectrum at room temperature of the particles of Fig. 4a, 0.0504 g mixed with 0.203 g of CGW paste, and excited at 600 nm. The fluorescence is resolved into four components (solid traces): 673 nm (B=23 nm) 21.4%, 688(22) 25.7%, 706(20) 4.6%, and 733(58) 48.3%. Their sum is shown as a dashed trace, and observed intensities as open circles. On cooling to 77 K, the strongest band is at 688 nm.

2.40 μmol g^{-1} and $[4\text{-NPMA}]_p$=3.50 μmol g^{-1} was similarly resolved, but the composition (656 nm (24 nm) 32.4%, 665.5(20) 24.2%, 673.5(18) 25.8%, 685(17) 15.3%, 697.5(13) 2.4%) indicates less monomeric component and more of all the others.

The fluorescence spectra of these preparations are markedly broadened and red-shifted, even at room temperature, compared to those with 2-NPMA (Fig. 3b). A resolution into four bands is presented in Fig. 4b. In

TABLE 1. ANALYSIS OF ABSORPTION AND FLUORESCENCE SPECTRA OF CHLOROPHYLL a WITH 3-NPMA ON POLYETHYLENE–TETRADECANE PARTICLES

$[Chl]_p$[a] / μmol g^{-1}	$[3\text{-NPMA}]_p$ / μmol g^{-1}	$[3\text{-NPMA}]_p$ / $[Chl]_p$	λ/nm (B/nm)	%	λ/nm (B/nm)	%	λ/nm (B/nm)	%	λ/nm (B/nm)	%	λ/nm (B/nm)	%	λ/nm (B/nm)	%
Absorption spectra														
0.146	1.09	7.47	653 (18)	22.2	664.5 (16)	36.3	674 (16)	29.4	683 (14)	8.9	692 (13)	2.9	703 (8)	0.3
0.252	1.31	5.19	653 (18)	21.0	664.5 (16)	37.2	674 (16)	29.5	683 (14)	9.1	692 (13)	3.0	703 (8)	0.2
0.875	>8	>9	653 (18)	19.3	664.5 (16)	36.0	674 (16)	29.7	682.5 (14)	10.4	692 (13)	4.0	703 (8)	0.6
0.983	2.25	2.29	653 (18)	18.5	664.5 (16)	34.7	674 (16)	29.7	682.5 (14)	12.5	691.5 (11)	3.8	703 (8)	0.7
1.47	2.84	1.93	653 (18)	19.7	664.5 (16)	31.3	674 (16)	31.1	682.5 (14)	13.6	692 (11)	3.9	703 (8)	0.4
2.245	5.93	2.64	653 (18)	18.8	664.5 (16)	28.6	674 (16)	30.8	682.5 (14)	15.0	691.5 (13)	6.2	703 (8)	0.7
2.38	7.14	3.00	653 (18)	18.8	664.5 (16)	28.1	674 (16)	30.6	682.5 (14)	15.0	691.5 (13)	6.6	703 (8)	0.9
Fluorescence spectra														
0.146	1.09	7.47	670.7 (19)	46.9	687.5 (16)	11.3	700.5 (16)	8.7	710 (10)	0.9	724 (30)	26.1	748 (24)	6.1
0.405	6.60	16.3	670.5 (17)	45.3	686 (15)	13.6	700 (18)	7.9	—		727 (40)	33.2	b)	
0.875	>8	>9	671 (21)	34.3	688 (15)	11.9	700.5 (16)	8.4	710 (10)	0.3	724.5 (38)	39.9	756 (30)	5.2
2.245	5.93	2.64	671 (18)	28.5	688 (15)	20.4	700.5 (16)	10.8	711 (10)	0.4	722.5 (36)	33.6	766 (26)	6.2
2.38	7.14	3.00	670.5 (17)	32.0	687.5 (13)	14.8	699.5 (16)	13.5	711 (10)	0.5	722 (34)	39.2	b)	

a) The columns list the chlorophyll and 3-NPMA contents of the particles, the ratio of these quantities, and data for the component bands into which each spectrum was analyzed. These data are the peak wavelength (λ) and bandwidth (B) at half peak height, and the percent of the total integrated absorption or fluorescence occupied by the component band. Sometimes a small component at 741nm was present in the absorption spectrum; this was omitted from the analysis. b) A small component around 760 nm was omitted from the calculation because of excessively noisy trace in this region.

the red region, the component at 688 nm is stronger than the presumed monomer component at 673 nm. The broad band centered at 733 nm is probably complex, and contains vibrational satellites of the 673 and 688 nm bands, but appears too strong to be accounted for entirely this way.

On cooling the sample of Fig. 4b to 77 K, the 673 nm fluorescence is suppressed and the 688 nm component remains as the leading band in the spectrum. In the more concentrated sample with $[Chl]_p=2.40$ μmol g^{-1}, the leading band peak at 77 K is at 691 nm.

N-*(3-Pyridyl)myristamide.* Spectra with this isomer were the most complex of the three. A total of 15 preparations were examined ranging in chlorophyll content from $[Chl]_p=0.146$ to 2.38 μmol g^{-1}, and in initial 3-NPMA concentration (in 90% methanol) from

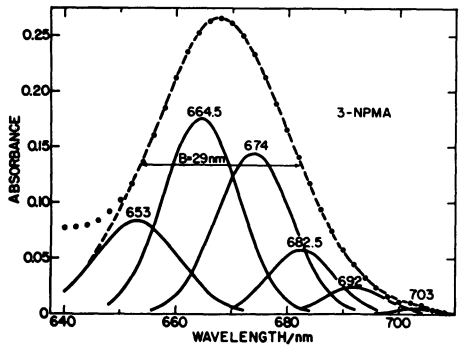

Fig. 5a. Absorption spectrum of particles containing chlorophyll (0.875 μmol g^{-1}) and at least 8 μmol g^{-1} 3-NPMA (see Table 1), 0.0085 g mixed with 0.577 g sucrose–cellulose paste. The broad red band is resolved into six components: 653 nm ($B=18$ nm) 19.3%, 664.5 (16) 36.0%, 674(16) 29.7%, 682.5(14) 10.4%, 692(13) 4.0%, and 703(8) 0.6%. The last three components are identified in numerous second derivative spectra, but the small 703 nm component may belong to the paste background. The sum of the components is shown as a dashed trace, and observed absorbances as open circles.

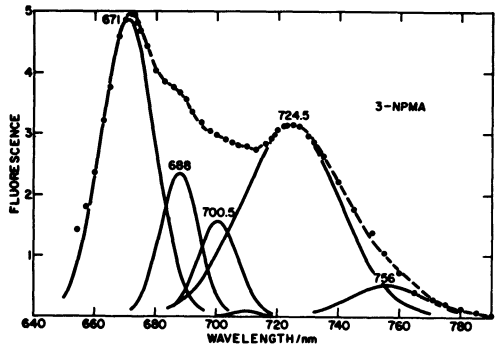

Fig. 5b. Fluorescence spectrum at room temperature of the particles of Fig. 5a, mixed with CGW paste, and excited at 600 nm. The spectrum is resolved into six components (solid traces): 671 nm ($B=21$ nm) 34.3%, 688(15) 11.9%, 700.5(16) 8.4%, 710(10) 0.3%, 724.5 (38) 39.0%, and 756(30) 5.2%. Their sum is shown as a dashed trace, and observed intensities as open circles. For fluorescence resolutions at other chlorophyll and 3-NPMA concentrations, see Table 1.

0.625 to 20 mM. Above 10 mM initial concentration the solubility limit of 3-NPMA in 75% methanol was exceeded, and crystals of the amide were to some extent collected with the particles, a circumstance that seems to have had no effect whatever on the visible spectrum of adsorbed chlorophyll. The red band is broadened, as it is in spectra with 4-NPMA, and the peak position varies with $[Chl]_p$ in the range 665—670 nm. The second derivative spectra were rather complex. Especially in relatively concentrated suspensions most preparations showed a trough or shoulder near 684 nm; several of these, particularly those with a low $[3\text{-NPMA}]_p/[Chl]_p$ ratio, also showed a sharp trough near 692 nm. Only when the initial 3-NPMA concentration was less than 2.5 mM, or $[3\text{-NPMA}]_p/[Chl]_p<2$, was there a significant amount of the 741 nm chlorophyll species in the particles.

Acceptable resolution of absorption spectra was obtained with six components of almost invariable position and bandwidth at 653, 664.5, 674, 682.5, 692, and 703 nm. The 682.5 and 692 nm components were located approximately by second derivative spectroscopy, as just mentioned. The first three components were required to represent the broadening of the main part of the red band, as in the resolution of spectra with 4-NPMA. The 703 nm component is always small and may belong to the paste background. Results for several of the samples are compiled in Table 1, and one of the resolutions is illustrated in Fig. 5a. The resolution is really rather similar over the concentration ranges covered. However, the 682.5 and 692 nm component contributions increase by a factor of about 2 as $[Chl]_p$ increases, largely at the expense of the presumed monomeric component at 664.5 nm.

Fluorescence spectra were consistently resolved into six bands, near 671, 688, 700, 710, and 724 nm, and one in the range 748—766 nm. The 710 nm component is insignificant. Some resolutions are compiled in Table 1, and the one corresponding to the absorption spectrum of Fig. 5a is shown in Fig. 5b. The strongest fluorescence component at low $[Chl]_p$ is the 671 nm band, which evidently belongs to monomeric chlorophyll. The 688 nm component, which appears as a shoulder in Fig. 5b, appears as a peak in the $[Chl]_p=2.245$ μmol g^{-1} preparation, higher than the 671 nm peak and clearly set apart from it. The 700 and 724 nm bands also tend to increase somewhat with $[Chl]_p$, at the expense of monomer fluorescence.

On quickly cooling the preparation with smallest $[Chl]_p$ to 77 K, the main fluorescence band peak appeared at 685 nm; in the other preparations, the band appeared in the range 693—700 nm, generally near 695 nm.

Discussion

It has thus been possible to resolve both the absorption and fluorescence spectra of adsorbed chlorophyll into minimal, consistent sets of Gaussian components characteristic of the amphiphile adsorbed with it. The next step in comparison of amphiphiles is to determine, if possible, correspondences between absorption and fluorescence components (Table 2). This process is

TABLE 2. CORRELATION OF ABSORPTION AND FLUORESCENCE SPECTRA OF CHLOROPHYLL a ADSORBED TO POLYETHYLENE–TETRADECANE PARTICLES WITH VARIOUS AMIDE-CONTAINING AMPHIPHILES

Amphiphile[a]	Absorption components[b]			Fluorescence[c] by Eq. 5	Fluorescence components[b]			
	λ/nm	(B/nm)	%[d]	λ/nm	λ/nm	(B/nm)		%[d]
OCC	665.8	(24)	100	677	680	(23)		57.3
					702	(20)		8.9
					732	(40)		33.8
2-NPMA	666	(24)	92.5[e]	677	674.5	(21)		36.1
	673.5		0	685 ?	683—7		(77K)	
	684	(24)	7.5	695	693	(23)		15.2
					705	(16)		2.4
					726.5	(38)		43.7
					752	(24)		2.5
MAn	655	(20)	11.5[f]					
	665	(20)	34.8	673	676	(24)		52.1
	674	(20)	37.5	682 ?	686		(77K)	
	682.5	(20)	16.2	690	697.5	(20)		9.4
					723.5	(40)		33.3
					765	(32)		5.2
4-NPMA	656	(24)	24.8					
	666	(20)	37.0	674	673	(23)		21.4
	673.5	(18)	23.6	680				
	684	(17)	13.2	690	688	(22)		25.7
	697.5	(13)	1.4	701	706	(20)		4.6
					733	(58)		48.3
3-NPMA	653	(18)	19.3					
	664.5	(16)	36.0	669.5	671	(21)		34.3
	674	(16)	29.7	679				
	682.5	(14)	10.4	686.5	688	(15)		11.9
	692	(13)	4.0	694.5	695		(77K)	
	703	(8)	0.6		700.5	(16)		8.4
					710	(10)		0.3
					724.5	(38)		39.9
					756	(30)		5.2
DMMA[g]	661.5	(20)	43.9	669.5	670			
	674	(20)	37.9	682	681			
	683	(20)	1.4	—				
	689	(20)	16.8	697	695—700		(77K)	
					705		(77K)	
					725			

a) Abbreviations: OCC: Chlorophyll particles mixed with 1-octanol–Carbowax–cellulose paste; MAn: myristanilide; NPMA: *N*-pyridylmyristamide; DMMA: *N,N*-dimethylmyristamide. b) Absorption spectra of Figs. 1, 3a—5a and of MAn in a paste of 6 : 10 : 3 Ficoll : glycerol : cellulose. All fluorescence spectra were recorded on samples in CGW paste. The composition of the paste has little effect on the spectral properties of the particles. Components marked (77K) have been identified with certainty only at a low temperature usually as the leading band of the fluorescence spectra. c) Calculated from the Stepanov theory of spectral band shape.[9,10] Dashed lines connect calculated band positions with most probably corresponding observed positions. d) Percentages given for typical spectra of Figs. 1, 3—5 or as noted; $[Chl]_p$ *ca.* 1 μmol g^{-1} and 741 nm species absent. e) An alternative analysis gave: 656 nm (17.2%), 665.5 (53.9%), 674.5 (24.3%), 690 (4.6%), all with B=20 nm. This analysis accommodates the presence of a 673.5 nm band at low $[2\text{-NPMA}]_p$ and perhaps the strength of the fluorescence band at 726.5 nm (see Discussion). f) A resolution into three bands: 658 nm (19.6%), 671 (64.7%), and 680.5 (15.7%) all with B=24 nm gave an acceptable fit but does not correlate well with the fluorescence spectrum. g) Spectra recorded and analyzed as reported in (I); a slightly better resolution might have been achieved with an additional band near 653 nm. The 683 nm absorption component is sensitive to the value of B chosen and is not present with certainty within the accuracy of the analysis. The 705 nm component in fluorescence, and at 77 K, which is strong only in preparations with low $[DMMA]_p/[Chl]_p$ is unique to this amphiphile.

assisted by a relation derived from Stepanov theory between the frequencies ν_M^{abs} and ν_M^{flu} of corresponding absorption and fluorescence band maxima, Eq. 5,[9]

$$\nu_M^{abs} - \nu_M^{flu} = B^2/8(\ln 2)kT, \quad (5)$$

which has been shown to be valid for chlorophyll in solution.[10] The relation will be accurate unless there is substantial rearrangement in the excited state before emission, or variations in the molecular environment

which give rise to heterogeneous band broadening are preserved during the lifetime of the excited state. Fluorescence band positions were calculated for several of the absorption band components by Eq. 5 and are liested next to them in Table 2. These predicted positions are connected by dashed lines to observed bands to which they most likely correspond.

The absorption and fluorescence components belonging to monomeric chlorophyll bound to the NPMA's and MAn are located in the ranges 664.5—666 nm and 671—676 nm; agreement between positions predicted by Eq. 5 and assigned fluorescence bands is satisfactory. The three NPMA isomers also have absorption band components at 682.5 nm (3-NPMA) or 684 nm (2- and 4-NPMA) which are evidently related to fluorescence components at 688 nm (3- and 4-NPMA) or 693 nm (2-NPMA). The agreement between predicted and observed positions is again quite good. An analogous pair of bands for MAn was not obvious.

Acceptable resolution of absorption spectra of 3- and 4-NPMA, probably of MAn, and perhaps of 2-NPMA, required a pair of components on either side of the monomer component, *e.g.*, at 656 and 673.5 nm for 4-NPMA. Their positions suggest that they could be the result of exciton interaction in dimers similar to that of the cofacial covalently-linked pyrochlorophyllide dimer described by Bucks and Boxer.[11] Alternatively, they might represent heterogeneous broadening of the monomeric chlorophyll band, but if so, the broadening is not reflected in the fluorescence spectrum. We could not identify a fluorescence component, with the aid of Eq. 5, corresponding to either of these absorption components at room temperature in spectra with any of these four amphiphiles.

On the other hand, the fluorescence spectra with the NPMA's all contain a broad farred component at 726.5 nm (2-NPMA), 724.5 nm (3-NPMA), and 733 nm (4-NPMA) which is stronger than can be accounted for as vibrational satellites of shorter-wave fluorescence components, as assumed for chlorophyll in OCC. Indeed, chlorophyll in many other model systems shows a fluorescence band in this region.[2] Fluorescence in this region is usually ascribed to an absorption band in the 695—700 nm region, as in the example described by Hindman *et al.*[12] In none of our spectra have we been able to resolve an absorption band in this region broad enough to account for the farred emission. As was discussed in the case of DMMA, where a 725 nm emission band is prominent, a very weak but broad absorption band could escape detection, but it is also conceivable that the farred fluorescence is a kind of excimer emission, associated with absorption bands at much shorter wavelengths. It is tempting to associate the farred emission bands, which have no observed corresponding absorption bands, with the above-mentioned pair of absorption bands (*e.g.*, 656 and 673.5 nm), which have no corresponding fluorescence. The validity of such an assignment must be established by further experimentation.

Data for the DMMA system[2] are also transcribed in Table 2; it is evident that there is very good agreement between observed fluorescence band positions and those calculated from the absorption bands by Eq. 5.

However desirable it may be to assign structures to the associated chlorophyll species detected in these studies, it is rarely possible to do so on the basis of electronic spectra alone. Nevertheless, the nature of the system imposes some limitations on the kinds of association that can be imagined to exist. A discussion of structures reasonably proceeds from the following assumptions. (1) The chlorophyll molecules tend to float at or near the particle surface, with the phytyl groups directed toward the particle interior, and the porphyrin planes making an angle of about 50° to the surface, as they have been found to do in lecithin layers.[13] (2) The amphiphile will be similarly oriented at the particle surface, and will therefore bind primarily to the Mg from the underside of the porphyrin plane. (3) The *N*-substituent of the monosubstituted amides will be directed mainly *trans* to the myristoyl group.[14] (4) Because water is present in abundance during adsorption, the Mg and C(9) or ring carbonyl of chlorophyll will be bound to water (or possibly methanol) unless it is displaced by a stronger nucleophile or H-bond donor respectively.[7,15] (5) Established structures of chlorophyll hydrate species[16] and anhydrous chlorophyll oligomers[17] are valid models for chlorophyll association and its spectral manifestations.

It is clear, through earlier work with DMMA and other amphiphilic amides, that these compounds act as nucleophiles toward the Mg of chlorophyll, and thus keep most of the pigment in a monomeric state.[1,2] The amphiphiles used in the present work (except DPB) are also potentially capable of ligating Mg through their amide carbonyl groups. The monosubstituted amides (but not DMMA) can also form hydrogen bonds with carbonyl groups of chlorophyll. The NPMA's, but not MAn, are potentially able to bind to Mg through the pyridine function as well as through the carbonyl. Finally, since all of these functional groups are normally bound to water in aqueous systems, water may serve as an intermediate link in any of these connections.

The results of Table 2, taken as a whole, suggest that MAn and 2-NPMA behave somewhat differently from 3- and 4-NPMA. In spite of their greater solubility in the particles (or perhaps because of it), MAn and 2-NPMA interact rather weakly with chlorophyll, give absorption spectra which are somewhat broadened but not clearly structured, and show fluorescence in which monomer emission predominates. In contrast, 3- and 4-NPMA appear confined to the particle surface, where they interact strongly with chlorophyll, produce absorption bands which are distinctly structured and broadened, especially on the long-wavelength side, and show fluorescence spectra with important contributions from associated species. Models of these amides suggest that direct ligation of the carbonyl group to Mg of chlorophyll is somewhat hindered by the aromatic substituent, except perhaps in 3-NPMA. However, direct ligation of the pyridine nitrogen to Mg is unhindered in 3- and 4-NPMA, whereas it is almost impossible in 2-NPMA. It therefore seems likely that 3- and 4-NPMA are bound to the underside of the porphyrin plane through pyridine nitrogen, whereas 2-

NPMA and MAn are bound through the amide carbonyl, directly or perhaps through water. The binding of amide carbonyl in DMMA to Mg does not appear to be hindered.

According to Table 2, the three NPMA's and perhaps MAn give absorption spectral components in the range 682.5—684 nm, which are associated with fluorescence components in the range 688—693 nm. Particles with DMMA lack these components, within the sensitivity of the analysis. Since only the monosubstituted amides could form hydrogen bonds directly to chlorophyll carbonyls, it is possible that the associated species responsible for these bands are linked by ligation of the amide carbonyl or pyridine group to the Mg of one chlorophyll, and by a hydrogen bond from the amide nitrogen to the ring carbonyl of another. The monosubstituted amide thus acts as a bifunctional linking agent between two chlorophylls, much as simpler compounds such as alcohols do in solution at low temperature.[7] 3- and 4-NPMA form the strongest associations of this type. In this sort of association, the angle between the chlorophyll porphyrin planes is not well defined but tends to be rather large.

When a molecule of DMMA is bound through the amide carbonyl to the underside of one chlorophyll molecule, there is no functionality remaining by which it can link to another. However, chlorophyll adsorbed at high density to particles with DMMA does show bands of definite associated species at 674 and 689 nm. Construction of models, subject to the considerations outlined above, shows that the most likely way to link two chlorophyll molecules together is through a third DMMA molecule, bound to hydrated Mg on the upper side of one chlorophyll molecule and to the hydrated ring carbonyl group of the other. In this structure, the amide carbonyl is hydrogen-bonded to two waters at once, which is plausible because in the presence of water, amide carbonyls tend to be bound to two water molecules anyway.[18] The chlorophyll planes tend to be intermediate between parallel and perpendicular in this construction. If two chlorophyll molecules so connected produce the 674 nm absorption band component, three or more connected in series might give rise to the 689 nm component.

The four monosubstituted amides could link chlorophylls together in the same way, with one change: the amides could form hydrogen bonds directly from NH to chlorophyll carbonyl. The inequivalence of the linked chlorophyll molecules could be conductive to charge separation, as proposed by Yuen *et al.*,[19] and thus account for the farred band of fluorescence for which a charge-transfer excimer nature has been suggested.

The structures described above must be considered tentative until they can be supported by evidence bearing more directly on the nature of the linkages, such as resonance Raman spectroscopy. More important than the exact structures is that in these systems with closely related amphiphiles, the nature of chlorophyll association is conditioned by the structure of the amphiphile, and that the associated species are for the most part fluorescent.

This work was supported in part by Grant No. DE-FG01-80 ER10563 from the U. S. Department of Energy. We thank Dr. John W. McDonald for the C-H-N analyses, and Mr. Elwood R. Shaw for the synthesis of myristanilide. This is Contribution No. 802 from the Charles F. Kettering Research Laboratory.

References

1) G. R. Seely, "Chlorophyll Organization and Energy Transfer in Photosynthesis," Ciba Foundation Symposium 61 (new series), Excerpta Medica, Amsterdam (1979), pp. 41—59; *Biotechnol. Bioeng. Symp.* No. 8, 473—481 (1978); G. R. Seely and A. M. Rutkoski, "Photosynthesis I. Photophysical Processes-Membrane Energization," ed by G. Akoyunoglou, Balaban Int. Sci. Serv., Philadelphia (1981), pp. 213—221.

2) a) G. R. Seely, A. M. Rutkoski, Y. Kusumoto, V. Senthilathipan, and E. R. Shaw, *Photochem. Photobiol.*, **36**, 633 (1982); b) Y. Kusumoto, V. Senthilathipan, and G. R. Seely, *Photochem. Photobiol.*, in press (1983).

3) L. W. Deady and D. C. Stillman, *Aust. J. Chem.*, **32**, 381 (1979).

4) H. Sugeta, *Bull. Chem. Soc. Jpn.*, **54**, 3706 (1981).

5) W. L. Butler, *J. Opt. Soc. Am.*, **52**, 292 (1962).

6) G. R. Seely and R. G. Jensen, *Spectrochim. Acta*, **21**, 1835 (1965).

7) T. M. Cotton, P. A. Loach, J. J. Katz, and K. Ballschmiter, *Photochem. Photobiol.*, **27**, 735 (1978).

8) F. K. Fong, M. Kusunoki, L. Galloway, J. G. Matthews, F. E. Lytle, A. J. Hoff, and F. A. Brinkmann, *J. Am. Chem. Soc.*, **104**, 2759 (1982); V. Karg, P. Kis, and G. Nauer, *Bioelectrochem. Bioenerg.*, **8**, 691 (1981); K. Uehara, Y. Nakajima, M. Yonezawa, and M. Tanaka, *Chem. Lett.*, **1981**, 1643; I. Inamura K. Toki, T. Araki, and H. Ochiai, *ibid.*, **1980**, 1481; other references cited in Ref. 2a.

9) L. P. Kazachenko, *Opt. Spectrosc.*, **18**, 397 (1965).

10) F. F. Litvin and I. N. Stadnichuk, *Biofizika*, **24**, 651 (1979) (*Biophysics*, p. 671).

11) R. R. Bucks and S. G. Boxer, *J. Am. Chem. Soc.*, **104**, 340 (1982).

12) J. C. Hindman, R. Kugel, M. R. Wasielewski, and J. J. Katz, *Proc. Natl. Acad. Sci. U.S.A.*, **75**, 2076 (1978).

13) R. J. Cherry, K. Hsu, and D. Chapman, *Biochim. Biophys. Acta*, **267**, 512 (1972); A. J. Hoff, *Photochem. Photobiol.* **19**, 51 (1974); F. Podo, J. E. Cain, and J. K. Blasie, *Biochim. Biophys. Acta*, **419**, 19 (1976).

14) L. A. LaPlanche and M. T. Rogers, *J. Am. Chem. Soc.*, **86**, 337 (1964).

15) K. Ballschmiter and J. J. Katz, *J. Am. Chem. Soc.*, **91**, 2661 (1969).

16) L. L. Shipman and J. J. Katz, *J. Phys. Chem.*, **81**, 577 (1977); C. Kratky and J. D. Dunitz, *J. Mol. Biol.*, **113**, 431 (1977).

17) L. L. Shipman, T. M. Cotton, J. R. Norris, and J. J. Katz, *J. Am. Chem. Soc.*, **98**, 8222 (1976).

18) J. N. Spencer, S. K. Berger, C. R. Powell, B. D. Henning, G. S. Furman, W. M. Loffredo, E. M. Rydberg, R. A. Neubert, C. E. Shoop, and D.N. Blauch, *J. Phys. Chem.*, **85**, 1236 (1981).

19) M. J. Yuen, L. L. Shipman, J. J. Katz, and J. C. Hindmann, *Photochem. Photobiol.*, **32**, 281 (1980).